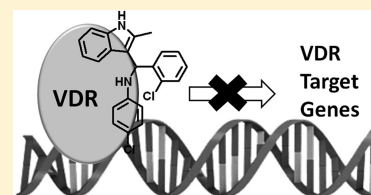


Discovery of the First Irreversible Small Molecule Inhibitors of the Interaction between the Vitamin D Receptor and Coactivators

Premchendar Nandhikonda,^{†,||} Wen Z. Lynt,^{†,||} Megan M. McCallum,[†] Tahniyath Ara,[†] Athena M. Baranowski,[†] Nina Y. Yuan,[†] Dana Pearson,[†] Daniel D. Bikle,[‡] R. Kiplin Guy,[§] and Leggy A. Arnold^{*,†}[†]Department of Chemistry and Biochemistry, University of Wisconsin-Milwaukee, Milwaukee, Wisconsin 53211, United States[‡]Endocrine Research Unit, Department of Medicine, Veterans Affairs Medical Center, San Francisco, California 94121, United States[§]Department of Chemical Biology and Therapeutics, St. Jude Children's Research Hospital, Memphis, Tennessee 38105, United States

S Supporting Information

ABSTRACT: The vitamin D receptor (VDR) is a nuclear hormone receptor that regulates cell proliferation, cell differentiation, and calcium homeostasis. The receptor is activated by vitamin D analogues that induce the disruption of VDR–corepressor binding and promote VDR–coactivator interactions. The interactions between VDR and coregulators are essential for VDR-mediated transcription. Small molecule inhibition of VDR–coregulator binding represents an alternative method to the traditional ligand-based approach in order to modulate the expression of VDR target genes. A high throughput fluorescence polarization screen that quantifies the inhibition of binding between VDR and a fluorescently labeled steroid receptor coactivator 2 peptide was applied to discover the new small molecule VDR–coactivator inhibitors, 3-indolylmethanamines. Structure–activity relationship studies with 3-indolylmethanamine analogues were used to determine their mode of VDR-binding and to produce the first VDR-selective and irreversible VDR–coactivator inhibitors with the ability to regulate the transcription of the human VDR target gene *TRPV6*.



■ INTRODUCTION

The vitamin D receptor (VDR) is a ligand-activated transcription factor that belongs to the nuclear receptor (NR) superfamily. VDR binds to its endogenous ligand, 1,25-dihydroxyvitamin D₃ (1,25-(OH)₂D₃), with high affinity,¹ mediating the modulation of genes responsible for cell differentiation, proliferation, and calcium homeostasis.² On the basis of its biological function, the VDR has been identified as an important pharmaceutical target for the treatment of metabolic disorders, skin diseases, cancer, autoimmune diseases, and cardiovascular diseases.³ The receptor contains several functional domains, including a DNA binding domain (VDR-DBD) and a ligand-binding domain (VDR-LBD), which mediates ligand-dependent gene regulation.⁴ VDR binds DNA as a heterodimer with the retinoid X receptor (RXR).⁵ In the unliganded state, VDR is associated with corepressor proteins, which repress transcription of VDR target genes.⁶ In the presence of 1,25-(OH)₂D₃, the VDR-LBD undergoes a conformational change. This conformational change prevents corepressor binding and permits interactions with coactivator proteins, resulting in the formation of a multiprotein complex that activates VDR-mediated transcription.⁷

VDR ligand agonists have been developed to treat metabolic bone diseases and proliferative skin disorders.³ In contrast to the large number of reported VDR agonist, only a limited number of VDR ligand antagonists have been described with the ability to allosterically inhibit the interactions between VDR

and its coactivators.⁸ All of these antagonists are based on the secosteroid scaffold of 1,25-(OH)₂D₃. A different approach to modulate gene regulation that is mediated by VDR represents the disruption of VDR–coregulator binding in the presence of 1,25-(OH)₂D₃. Small molecule NR–coactivator inhibitors have been discovered for the estrogen receptor, thyroid receptor, androgen receptor, and pregnane X receptor using rational design and high throughput screening (HTS).⁹ Mita et al. introduced the first reversible small molecule VDR–coactivator inhibitors.¹⁰ These compounds inhibited both VDR-mediated and estrogen receptor β -mediated transcription. Thus, highly potent and selective VDR–coactivator inhibitors are still missing. It is expected that these compounds can be applied as molecular probes to identify the biological functions of VDR–coactivator interactions. Herein, we describe the first HTS campaign that identified small molecule VDR–coactivator inhibitors and their evaluation using carefully selected secondary assays. One class of inhibitors were investigated in regard to their mode of VDR binding, selectivity, and SARs that resulted in the identification of the first irreversible and highly selective VDR–coactivator inhibitor with the ability to modulate VDR-mediated transcription.

Received: January 27, 2012

Published: May 7, 2012

Table 1. Summary of Biophysical and Biochemical Properties of Validated VDR–SRC2-3 Inhibitors

compd	% purity ^a	solubility (μM) ^b	permeability, ^c $\log(P_e)$ (cm/s)	VDR–SRC2-3 inhibition, IC_{50} (μM) ^d	inhibition of transcription (%) ^e		toxicity (%) ^g	
					62.5 μM	20.8 μM	62.5 μM	20.8 μM
1	93.0	0.1	−7.86	3.3	6.0 ^f		3.1 ^f	
2	89.8	273.3	−6.55	4.0	5.5 ^f		4.7 ^f	
3	89.2	0.7	−8.22	5.9	5.7 ^f		3.6 ^f	
4	94.7	0.2	−7.93	8.6	11.5 ^f		7.6 ^f	
5	88.6	218.7	−7.70	13.8	6.8 ^f		5.5 ^f	
7	95.2	21.9	−6.60	7.1	1.6 ^f		2.4 ^f	
8	96.1	49.9	−6.67	8.1	5.3 ^f		12.5 ^f	
9	94.5	17.6	−6.78	6.9	6.2 ^f		16.7 ^f	
10	99.6	34.2	−6.36	22.3	2.6 ^f		7.7 ^f	
11	42.8	342.0	−6.25	9.6	100	90	11	42.8
12	58.0	422.6	−6.10	27.7	100	10	12	58.0
13	65.6	403.3	−6.12	30.3	100	0	13	65.6
14	64.9	132.5	−6.11	14.1	100	10	14	64.9
15	84.1	84.6	−6.01	17.3	100	90	15	84.1
16	78.5	468.7	−6.05	28.9	100	10	16	78.5
17	42.4	201.4	−6.12	15.4	9.1 ^f		18.0 ^f	
18	81.6	277.7	−6.01	25.1	100	0	18	81.6
19	79.1	427.8	−5.99	22.2	80	0	19	79.1
20	58.1	466.8	−8.71	21.6	100	60	20	58.1
21	41.6	453.9	−7.84	37.7	100	30	21	41.6
22	57.6	462.0	−7.83	10.5	10.6 ^f		13.5 ^f (partial 50%)	
23	99.2	576.0	−8.28	20.5	50	15	23	99.2
24	84.1	42.1	−6.29	28.0	80	20	24	84.1
25	87.1	15.3	−6.52	14.3	100	60	25	87.1
26	67.6	493.0	−7.48	13.7	0	0	26	67.6
27	93.2	338.8	−7.28	2.0	30	0	27	93.2
28	98.9	487.0	−6.78	10.5	100	10	28	98.9
29	34.4	377.4	−5.95	25.1	65	0	29	34.4

^aPurities were determined by high pressure liquid chromatography using a photodiode array, and identity was confirmed by mass spectrometry.

^bSolubilities were determined in phosphate buffered saline at pH 7.4. ^cPermeabilities were measured using the parallel artificial membrane permeation assay (PAMPA) at neutral pH (pH 7.4). The following permeability standards ($\log P_e$) were used: ranitidine (-8.02 ± 0.074 cm/s) low permeability, carbamazepine (-6.81 ± 0.0011 cm/s) medium permeability, and verapamil (-5.93 ± 0.015 cm/s) high permeability. The solubility and permeability assay conditions reflect conditions required for activity in cell-based assays. ^dA fluorescence polarization competition assay was carried out using VDR-LBD (1 μM), Alexa Fluor labeled peptide SRC2-3 (7 nM), VDR-agonist LG190178 (5 μM), and serially diluted small molecules. IC_{50} values were obtained by fitting data to the following equation: $Y = \text{Bottom} + (\text{Top} - \text{Bottom}) / (1 + 10^{(\log \text{IC}_{50} - X)(\text{HillSlope})})$ using three independent experiments in quadruplet. ^eVDR-mediated inhibition of transcription was carried out using a commercially available GeneBLazer (Invitrogen) assay. Data were normalized by signals observed for inactive and activated VDR ($\pm 1,25(\text{OH})_2\text{D}_3$). ^f $\text{IC}_{50}/\text{LD}_{50}$ values (μM) are given instead of percentages for highly active compounds using the following nonlinear regression equation: $Y = \text{Bottom} + (\text{Top} - \text{Bottom}) / (1 + 10^{(\log \text{IC}_{50} - X)(\text{HillSlope})})$ using three independent experiments in quadruplet. ^gToxicity was determined using CellTiter-Glo (Promega), and data were normalized by signal observed for living and dead cells (± 100 μM 3-dibutylamino-1-(4-hexylphenyl)propan-1-one).

RESULTS

The HTS was carried out using 384-well black polystyrene plates with 20 μL of assay reagent per well. This assay reagent included VDR-LBD (1 μM), LG190178 (5 μM), Alexa Fluor 647 labeled SRC2-3 (7.5 nM), and a selected small molecule from the screening library (30 μM). FP was measured after 3 h of incubation. Recently, we quantified the binding affinities between VDR-LBD and different coregulator peptides using the same technique and discovered that the third nuclear interaction domain (NID) of steroid receptor coactivator 2 (SRC2), called SRC2-3, has the strongest interaction with VDR among other coregulator peptides tested.¹¹ The study also showed that the binding affinities of these peptides were similar in the presence of either 1,25-(OH)₂D₃ or synthetic agonist LG190178.¹² Three-hundred different compounds were investigated per plate, which contained also the negative control, dimethyl sulfoxide (DMSO), and the positive control

compound 3-dibutylamino-1-(4-hexylphenyl)propan-1-one, which has been reported to inhibit the interaction between coactivator SRC2 and the thyroid receptor β^{13} and which inhibit the interaction between VDR and SRC2-3 (see Supporting Information). A far-red fluorescent label (Alexa Fluor 647, 630/685 nm) was used for SRC2-3 to minimize fluorescent interference by fluorescence quenching and aggregation of screening compounds. Two-hundred seventy-five thousand compounds were tested in the primary screening campaign at a single dosage of 30 μM . On the basis of the FP signal, 589 compounds exhibited more than 40% inhibition of the VDR–SRC2-3 interaction at that concentration and were less likely to bear structure elements of promiscuous aggregating molecules¹⁴ or electrophilic compounds.¹⁵ HTS evaluation of the frozen stock solutions of these compounds confirmed that 140 compounds exhibited a dose-dependent response with IC_{50} values of less than 40 μM . Further analyses

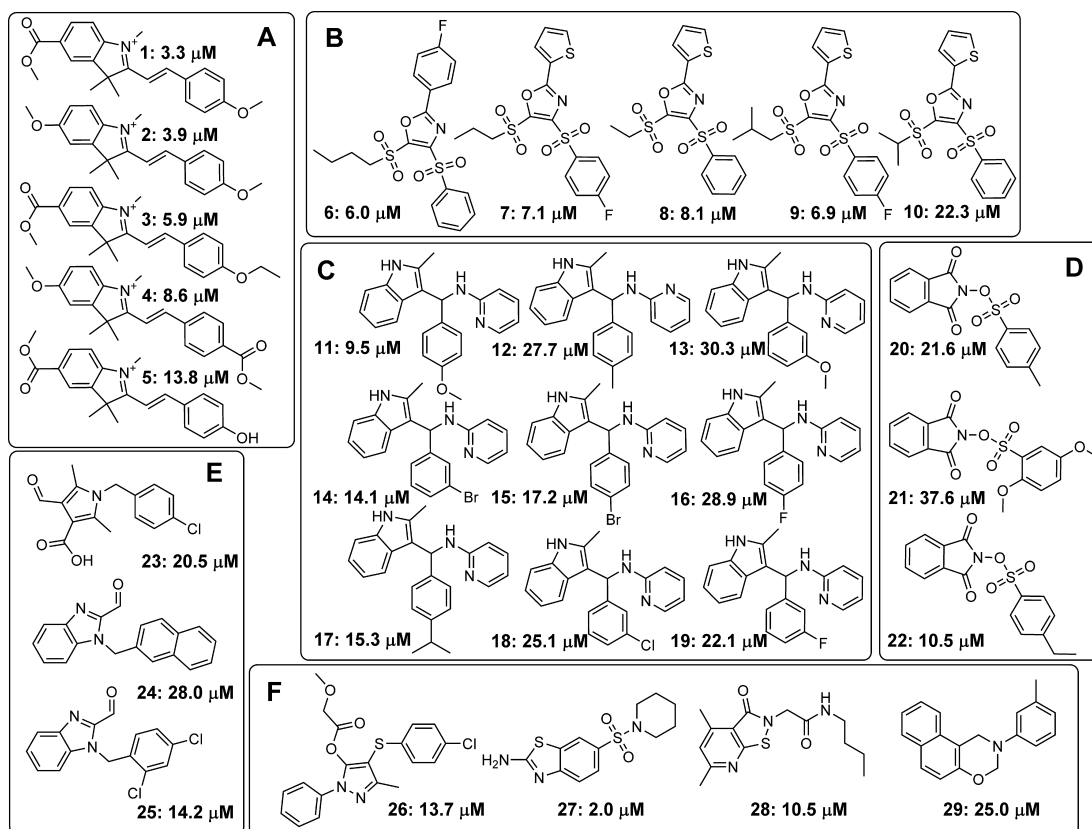


Figure 1. Hit structures from HTS for inhibitors of the interaction between VDR-LBD and fluorescently labeled peptide SRC2-3. Structures of validated hits are shown, grouped by chemotype, and annotated with IC_{50} values that were determined using a fluorescence polarization assay that employed VDR-LBD and fluorescently labeled peptide SRC2-3.

of these stock solutions were performed in HEK293 cells, which express a fusion protein of VDR-LBD and GAL4-DBD. It was determined that these cells induced the transcription of a β -lactamase reporter gene in the presence of $1,25\text{-(OH)}_2\text{D}_3$ (GeneBLazer, Invitrogen). Quantification of β -lactamase was accomplished by detecting the decrease of fluorescence resonance energy transfer (FRET) caused by the enzymatic cleavage of the β -lactam containing substrate, which was added after an incubation time of 24 h. The quantity of uncleaved substrate, which was determined by measuring the fluorescence emission at 447 nm, revealed that 48 of the 140 active compounds were able to regulate the VDR-mediated transcription of β -lactamase. Additionally, the abilities of these compounds to inhibit the interaction between VDR and $1,25\text{-(OH)}_2\text{D}_3$ were determined to exclude allosteric VDR-coactivator binding disruption through VDR ligand antagonism. The application of a VDR PolarScreen (Invitrogen) confirmed that none of the active compounds was able to replace labeled $1,25\text{-(OH)}_2\text{D}_3$.

The 48 compounds were then purchased as solids, dissolved in DMSO as a 10 mM solution, and analyzed by liquid chromatography–mass spectrometry (LC–MS) to determine purity and identity (Table 1). A subsequent dose–response analysis using the described FP assay determined that 29 of the 48 purchased compounds exhibited IC_{50} values of less than 40 μM . These compounds were divided into 6 groups, based on their scaffold similarity, and depicted in Figure 1 with their determined FP IC_{50} values.

Further characterizations were carried out, which include the determination of small molecule aqueous solubility, perme-

ability using PAMPA (parallel artificial membrane permeability), toxicity in HEK293T cells, and their ability to inhibit VDR-mediated transcription using the described GeneBLazer assay. The results are summarized in Table 1.

The 3-indolylmethanamines grouped in C showed the most promising characteristics, which included good to excellent solubility, high permeability, inhibition of VDR–SRC2-3 interaction at low micromolar concentrations, and the ability to inhibit VDR-mediated transcription in the range of 62.5–20.8 μM .

Selected analogues of 3-indolylmethanamines were regenerated in our laboratory in regard to the low purities and limited commercial availability of these compounds. In order to analyze the electronic effects of both aromatic substituents, we substituted the pyridine ring of the compounds depicted in Figure 1 with substituted phenyl groups as shown in Figure 2. For synthesis details, see Supporting Information. Three series of 3-indolylmethanamines were generated, including those bearing electron-donating and -accepting aromatic substituents (Figure 2).

The compounds were characterized using carefully selected biophysical and biochemical assays that are summarized in Table 2. The 2-chlorophenyl substituent was chosen for series 31 because 31a exhibits a higher activity (IC_{50}) and higher rate constant (k) in comparison with others members of group 30.

These assays included a VDR transcription assay that employed luminescence instead of FRET. The assay is based on the VDR-mediated transcription of a luciferase gene under control of the *CYP24A1* gene promoter.¹⁶ The gene product of *CYP24A1* is 24(R)-hydroxylase, which is responsible for the

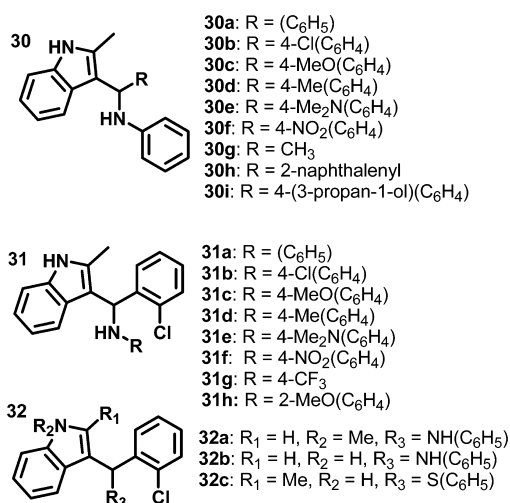


Figure 2. Structures of synthesized 3-indolylmethanamines.

catabolism of vitamin D analogues into their 24-hydroxylated species.¹⁷ CYP24A1 is highly and directly regulated by VDR.

The solubility of compounds from series 30 is excellent except those bearing a 2-chloroaryl or 2-naphthalenyl substituent (Table 2, compounds 31a and 30h). Molecules from series 31 and 32, which bear a 2-chloroaryl substituent,

also have lower solubility, ranging from 4.9 to 85 μ M. The permeability of all series 30–32 range from medium to high in comparison with drug standards carbamazepine ($\log P_e = -6.81$ cm/s, medium) and verapamil ($\log P_e = -5.93$ cm/s, high). Determination of the ability of 3-indolylmethanamines to inhibit the interaction between VDR and SRC2-3 resulted in similar IC₅₀ values, ranging from 27 to 44 μ M, for the majority of compounds after 3 h. Significantly higher IC₅₀ values were observed for compound 30g, bearing a methyl group (IC₅₀ = 104 μ M) instead of an aryl group, and compounds 30e, 31e, 31f, and 31g, bearing electron-withdrawing aromatic substituents. For the last four compounds, nonlinear fitting resulted in IC₅₀ values with high standard deviation caused by lack of saturation at higher compound concentrations (Table 2). Additionally, we observed loss of activity for 3-indolylmethanamines with the alkylation of the indole nitrogen (32a) or nitrogen–sulfur substitution (32c). Compound 32b, missing the 2-methylindole substituents, inhibited only 50% of the interaction between VDR and SRC2-3. The FP analysis of the VDR–coactivator inhibition reaction at different time points identified significant changes of inhibition in time. This prompted us to determine each compound's rate constant by fitting the data to first order dissociation kinetics (see Supporting Information). Small standard deviations support the application of this model and enabled us to identify large

Table 2. Summary of Biophysical and Biochemical Properties of 3-Indolylmethanamines

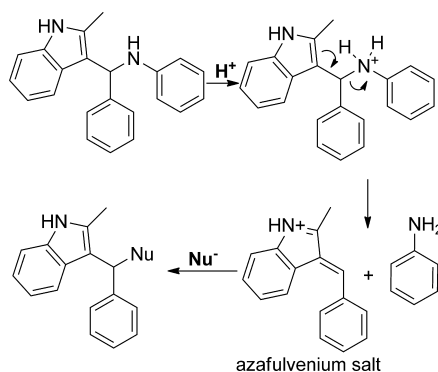
compd	solubility (μ M) ^a	permeability, ^b $\log(P_e)$ (cm/s)	VDR–SRC2-3 inhibition, IC ₅₀ (μ M) ^{c,g}	rate constant <i>k</i> for the dissociation of SRC2-3 from VDR (10 ⁻⁵) ^{d,g}	transcription inhibition, IC ₅₀ (μ M) ^e	toxicity LC ₅₀ (μ M) ^f
30a	252.9	-6.00	30.2 ± 4.8	45.1 ± 1.6	10.9 ± 2.8	15.3 ± 2.9
30b	93.9	-6.03	31.7 ± 4.3	34.2 ± 1.0	8.1 ± 1.7	14.6 ± 3.4
30c	237.5	-6.10	31.2 ± 3.2	88.0 ± 4.7	12.1 ± 1.8	17.2 ± 2.5
30d	175.1	-6.34	43.6 ± 7.8	35.7 ± 1.4	14.6 ± 2.5	21.7 ± 4.2
30e	157.7	-6.88	n.s.	2.0 ± 0.16	13.5 ± 1.3	25.8 ± 6.3
30f	117.6	-6.08	28.5 ± 4.5	6.7 ± 0.12	12.2 ± 2.4	16.2 ± 2.5
30g	189.0	-6.40	104.8 ± 15.2	1.8 ± 0.15	20.1 ± 5.2	37.4 ± 7.7
30h	67.3	-6.30	29.6 ± 3.1	14.2 ± 0.28	15.0 ± 2.4	20.8 ± 3.5
30i	503.4	-6.83	58.6 ± 8.1	2.3 ± 0.21	13.1 ± 2.5	31.4 ± 8.2
31a	31.6	-6.41	29.8 ± 4.5	38.6 ± 0.89	8.5 ± 1.8	12.6 ± 2.2
31b	68.0	-6.24	36.7 ± 5.1	4.5 ± 0.59	4.2 ± 1.9	11.6 ± 1.7
31c	84.2	-6.30	26.5 ± 3.4	39.1 ± 1.3	5.8 ± 2.1	12.1 ± 2.2
31d	35.9	-6.45	17.7 ± 3.2	23.7 ± 0.35	8.2 ± 1.5	12.7 ± 3.0
31e	21.0	-7.28	n.s.	0.87 ± 0.13	8.7 ± 1.5	19.4 ± 3.8
31f	4.9	-7.60	n.s.	1.2 ± 0.16	4.4 ± 1.1	11.0 ± 2.1
31g	n.d.	n.d.	n.s.	2.5 ± 0.07	24.0 ± 5.7	43.1 ± 9.1
31h	59.7	-6.22	24.3 ± 4.4	25.2 ± 0.36	8.6 ± 1.1	12.1 ± 2.7
32a	15.3	-6.58	n.o.	n.o.	>70	>70
32b	52.3	-6.51	20.3 ± 4.5 (partial)	1.4 ± 0.12	21.6 ± 3.3	>70
32c	11.8	-6.89	n.o.	n.o.	>70	>70

^aSolubilities were determined in phosphate buffered saline at pH 7.4. ^bPermeabilities were measured using the parallel artificial membrane permeation assay (PAMPA) at neutral pH (pH 7.4). The following permeability standards were used ($\log P_e$): ranitidine (-8.02 ± 0.074 cm/s) low permeability, carbamazepine (-6.81 ± 0.0011 cm/s) medium permeability, and verapamil (-5.93 ± 0.015 cm/s) high permeability. The solubility and permeability assay conditions reflect conditions required for activity in cell-based assays. ^cA fluorescence polarization competition assay was carried out using VDR-LBD (1 μ M), Alexa Fluor labeled peptide SRC2-3 (7 nM), VDR-agonist LG190178 (5 μ M), and serial diluted small molecules. IC₅₀ values were obtained by fitting data obtained after 3 h to the following equation: $Y = \text{Bottom} + (\text{Top} - \text{Bottom}) / (1 + 10^{(\log(\text{IC}_{50} - X) / \text{HillSlope}))}$ using three independent experiments in quadruplet. ^dA fluorescence polarization assay described under footnote ^c was monitored over time. Dissociation rate constants were obtained by linear fitting of $\ln(\text{mP})$ (fluorescence polarization) against time (first order kinetics). ^eHEK293T cells were transfected with CMV-VDR, a CYP24A1 promoter driven luciferase expression vector, and a *Renilla* luciferase control vector. The data were normalized to *Renilla* luciferase activity and by signals observed for inactive and activated VDR ($\pm 1,25(\text{OH})_2\text{D}_3$). ^fToxicity was determined based on signal observed for *Renilla* luciferase activity and normalized to signal observed for living and dead cells (± 100 μ M 3-dibutylamino-1-(4-hexylphenyl)propan-1-one, CBT358); ^gn.d. = not determined; n.s. = no saturation of signal at higher small molecule concentration (no reliable nonlinear fitting possible); n.o. = not observed.

reactivity differences between the 3-indolylmethanamines tested. As expected, we observed smaller rate constants for 3-indolylmethanamines with higher IC_{50} values of more than 44 μM (30e, 30g, 30i, 31e, 31f, and 31g). Four 3-indolylmethanamines (30f, 30h, 31b, and 32b) exhibited IC_{50} values in the range of 27–44 μM but showed relative small reaction rates. Interestingly, compound 31d, which has the lowest IC_{50} values, does not have the highest reaction rate. The ability of 3-indolylmethanamines to displace 1,25-(OH) $_2$ D $_3$ from VDR was determined by a commercially available FP assay (Polarscreen, Invitrogen) and excludes VDR ligand displacement by 3-indolylmethanamines, which can cause allosteric disruption of the VDR–coactivator interaction. None of the synthesized 3-indolylmethanamines were able to inhibit the interaction between labeled 1,25-(OH) $_2$ D $_3$ and VDR except compounds 30e and 30f, which exhibited weak inhibition at higher concentrations (see Supporting Information). Almost all 3-indolylmethanamines were able to inhibit the VDR-mediated transcription at lower micromolar concentrations except those that were not able to inhibit the interaction between VDR and SRC2-3 (Table 2, compounds 32a and 32c). We also observed significant cell toxicity caused by 3-indolylmethanamines at higher concentrations. The small difference between transcriptional inhibition and toxicity prompted us to use rt-PCR to determine the modulation of gene regulation in the presence of 3-indolylmethanamines.

The different reaction rates of the 3-indolylmethanamines and similar IC_{50} values indicate that these compounds are likely to react with VDR or SRC2-3 in an irreversible fashion. Indeed, it was reported that, especially under acidic conditions or elevated temperature, 3-indolylmethanamines underwent elimination reactions by breaking the carbon–nitrogen bonds and forming the corresponding azafulvenium salts (Scheme 1).¹⁸

Scheme 1. Proposed Mechanism of Action for 3-Indolylmethanamines



To discriminate which of the binding partners (VDR or SRC2-3) is alkylated by 3-indolylmethanamines, we incubated 31b for 3 h with either VDR or SRC2-3 followed by the addition of the other interaction partner that was SRC2-3 or VDR, respectively (Figure 3). The binding isotherm of each condition was different. Preincubation of 31b with SRC2-3 followed by the addition of VDR did not result in an alkylation reaction because the FP signal did not change with higher concentration of 31b. In contrast, preincubation of VDR with different 31b concentrations followed by the addition of SRC2-3 did result in a change of FP signal. The corresponding isotherm was similar to the inhibition observed for combining all reagents at the same time and measuring FP after 3 h.

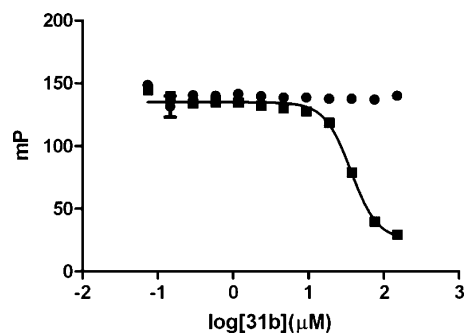


Figure 3. Identification of 31b's reaction partner. (●) Alexa Fluor-labeled SRC2-3 peptide (7 nM) was incubated for 3 h with different concentration of 31b followed by the addition of VDR-LBD (1 μM) and LG190178 (5 μM). Fluorescence polarization was detected after 5 min. (■) VDR-LBD (1 μM) and LG190178 (5 μM) were incubated for 3 h with different concentrations of 31b followed by the addition of Alexa Fluor labeled SRC2-3 peptide (7 nM). Fluorescence polarization was detected after 5 min.

The azafulvenium salts are reactive electrophiles that can undergo reactions with natural occurring nucleophiles such as cysteine residues of proteins. The wide range of reaction rates of the differently substituted 3-indolylmethanamines and the fact that these compounds are likely to react with VDR irreversibly prompted us to investigate the possibility of a linear free energy relationship between the alkylation of VDR measured by disruption of VDR–SRC2-3 binding and the electronic nature of different aromatic 3-indolylmethanamine substituents; therefore, $\log(k_x/k_0)$ was plotted against Hammett σ -values for the compounds of series 30 and 31 (Figure 4).¹⁹

A strong correlation was found for both series ($r^2 = 0.93$) with significant negative ρ -values, supporting the proposed mechanism that during the rate determining step, a positive charge is building up. Additionally, we observed that this reaction is less sensitive to substituents of compound series 30 ($\rho = -1.1$) than to substituents of compound series 31 ($\rho = -1.5$). This supports the fact that substituents of series 30 have a majorly inductive stabilizing effect, resulting in a smaller absolute ρ -value than substituents of compound series 31, which can stabilize the positive charge via resonance.

In water at a neutral pH, 3-indolylmethanamines were stable for 24 h, but reaction occurred when high concentrations of 2-mercaptoethanol (5 mM) were added. To determine the selectivity of 3-indolylmethanamine (31b) toward different nucleophiles, an FP assay of different concentrations of 2-mercaptoethanol was carried out (Figure 5).

Two effects were observed. First, the IC_{50} values for 31b under identical conditions increased with the amount of 2-mercaptoethanol from 36.8 μM (0.01 mM 2-mercaptoethanol) to 82.2 μM (100 mM 2-mercaptoethanol). Second, the efficacy of each isotherm decreased with increasing amount of 2-mercaptoethanol. These results show that VDR–SRC2-3 binding inhibition by 31b was only changed in the presence of more than a 1000-fold excess of an alternative nucleophile, such as 2-mercaptoethanol.

Small molecule target selectivity is very important, especially toward different NR–coactivator interactions. To determine the NR selectivity of 3-indolylmethanamines, five additional NR–coactivator interactions were investigated: androgen receptor AR–SRC2-3, thyroid receptor TR α –SRC2-2 and TR β –SRC2-2, estrogen receptor β (ER β)–SRC2-2, and peroxisome proliferator-activated receptor γ (PPAR γ)–DRIP2

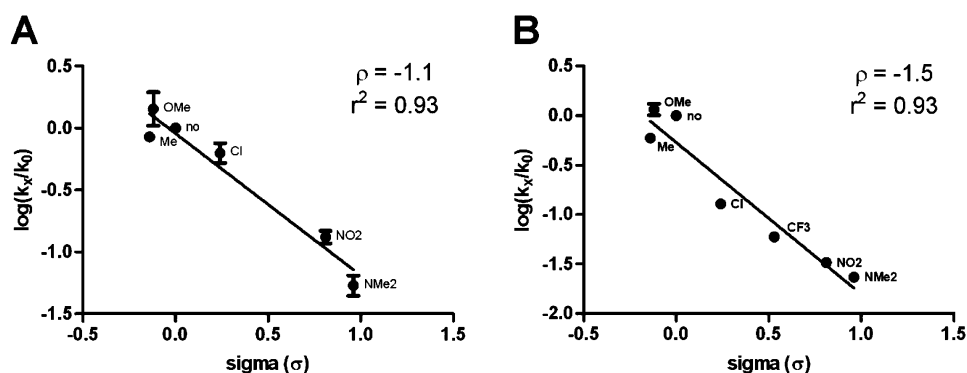


Figure 4. Linear free energy relationship between VDR–SRC2-3 inhibition and the electronic nature of 3-indolylmethanamines substituents: (A) series 30; (B) series 31. The $\log(k_x/k_0)$ values were calculated using rate constants given in Table 2, K_0 being the nonsubstituted compounds 30a and 31a. The σ -values were obtained from Ritchie et al. The ρ -values represent the slopes of the linear regressions with the corresponding r^2 values.

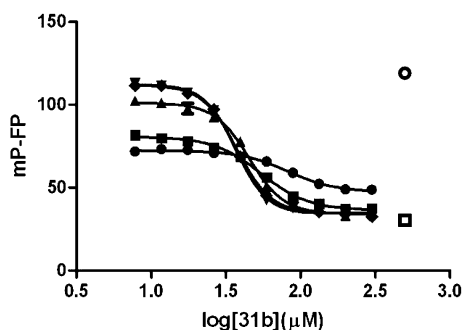


Figure 5. Influence of 2-mercaptoethanol for the inhibition of the VDR–SRC2-3 binding in the presence of 3-indolylmethanamine 31b. VDR–LBD (1 μM), LG190178 (5 μM), and Alexa Fluor labeled SRC2-3 peptide (7 nM) were incubated in the presence of different concentrations of 31b and in the absence and presence of different concentrations of 2-mercaptoethanol. Interactions between VDR and SRC2-3 were determined by fluorescence polarization: (○) DMSO (negative control), (□) 3-dibutylamino-1-(4-hexylphenyl)propan-1-one (positive control). 2-Mercaptoethanol concentrations (31b IC₅₀ values) were as follows: (●) 100 mM (82.2 ± 7.3 μM), (■) 10 mM (54.5 ± 3.1 μM), (▲) 1 mM (45.4 ± 2.0 μM), (▼) 0.1 mM (37.5 ± 1.1 μM), (◆) 0.01 mM (36.8 ± 0.5 μM).

(VDR-interacting protein 205). The quantification of these NR–coactivator interactions has been reported previously.²⁰ All 3-indolylmethanamines exclusively disrupted the VDR–SRC2-3 interaction, as depicted for compound 31b in Figure 6. The binding isotherms for all 3-indolylmethanamines are presented in the Supporting Information.

We also determined the abilities of 3-indolylmethanamines to inhibit different VDR–coregulator interactions. The quantification of interactions between VDR and coregulator peptides was reported recently.¹¹ Herein, we focused on three different coregulators, which include SRC2,²¹ DRIP205,²² and Hairless [Hr].²³ The results employing compound 31b are summarized in Figure 7.

Inhibition of binding was observed in the presence of 31b for VDR–SRC2-2, VDR–SRC2-3, and VDR–DRIP2 (Figure 7). The efficacy of these isotherms is dissimilar because of the different binding constants between VDR and SRC2-2 ($K_d = 1.7 \pm 0.2 \mu\text{M}$), VDR and SRC2-3 ($K_d = 0.93 \pm 0.17 \mu\text{M}$), and VDR and DRIP-2 ($K_d = 1.6 \pm 0.2 \mu\text{M}$). In comparison, the binding constant between VDR and SRC2-1 and VDR and Hr1 is greater than 5 μM and no inhibition by compound 31b was observed under these conditions. Interestingly, the IC₅₀ values

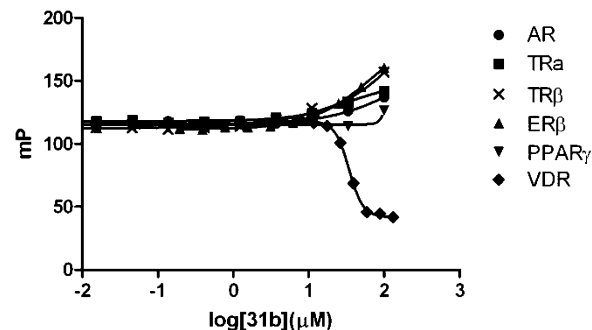


Figure 6. Nuclear receptor–coactivator binding studies in the presence of 3-indolylmethanamine 31b using fluorescence polarization. FP was detected at an excitation/emission wavelength of 595/615 nm. The conditions for different NRs are as follows: For AR, androgen receptor LBD (5 μM), Texas Red labeled SRC2-3 (7 nM), and dihydrotestosterone (5 μM) were incubated with small molecule for 3 h. For TRα, thyroid receptor α LBD (2 μM), Texas Red labeled SRC2-2 (7 nM), and triiodothyronine (1 μM) were incubated with small molecule for 3 h. For TRβ, thyroid receptor β LBD (0.8 μM), Texas Red labeled SRC2-2 (7 nM), and triiodothyronine (1 μM) were incubated with small molecule for 3 h. Estrogen receptor β (3 μM), Texas Red labeled SRC2-2 (5 nM), and estradiol (0.1 μM) were incubated with small molecule for 3 h. Peroxisome proliferator-activated receptor γ (5 μM), Texas Red labeled DRIP2 (7 nM), and rosiglitazone (5 μM) were incubated with small molecule for 3 h. For VDR, vitamin D receptor LBD (1 μM), Texas Red labeled SRC2-3 (7 nM), and LG190178 (5 μM) were incubated with small molecule for 3 h.

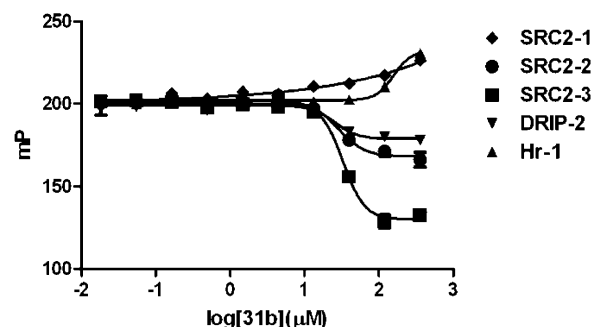


Figure 7. VDR–coactivator interactions in the presence of 31b using FP. VDR–LBD (1 μM), LG190178 (5 μM), and different Texas Red labeled coregulator peptides (7 nM) were incubated for 3 h in the presence of different concentrations of compound 31b.

of **31b** and for the VDR–SRC2-2, VDR–SRC2-3, and VDR–DRIP-2 interactions are very similar ($IC_{50} = 25.4 \pm 6.5 \mu\text{M}$, $IC_{50} = 28.5 \pm 6.9 \mu\text{M}$, and $IC_{50} = 33.1 \pm 3.4 \mu\text{M}$, respectively).

The ability of **31b** to partially inhibit the interaction between VDR and SRC2, containing all three SRC2 NIDs, was tested using a pull down assay (Figure 8). Control experiments

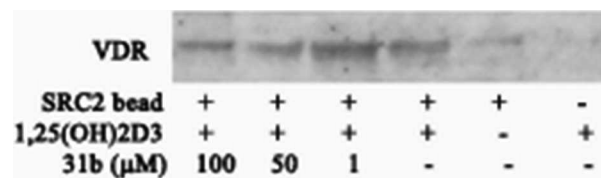


Figure 8. Western blot of in vitro binding reactions between SRC2 bearing all three NIDs and VDR-LBD in the presence of **31b**. Lanes 1–3 show different concentrations of **31b** in the presence of VDR, SRC2, and 1,25(OH)₂D₃. Lane 4 shows VDR, SRC2, and 1,25(OH)₂D₃. Lane 5 shows no ligand (1,25(OH)₂D₃), no coregulator (SRC2).

indicate that SRC2 bound to VDR in the presence of VDR ligand 1,25(OH)₂D₃ (Figure 8, lane 4) but not in the absence of 1,25(OH)₂D₃ (Figure 8, lane 5). The VDR–SRC2 interaction was blocked in a dose dependent manner by **31b** (Figure 8, lanes 1–3). Although significant inhibition of the VDR–SRC2 interaction was observed at 50 and 100 μM **31b**, a residual interaction between VDR and SRC2 could still be detected. Thus, the inhibition of the interaction between VDR and full length SRC2 by **31b** exhibits dose response dependence, similar to the SRC2-2 peptide binding study described above.

Additionally, we investigated the interaction between VDR and SRC2 in the presence of 3-indolylmethanamine or vehicle prior to the pull-down assay, to discriminate between **31b**–VDR and **31b**–SRC2 binding, respectively (Figure 9). VDR–

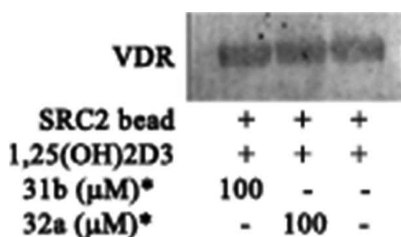


Figure 9. Western Blot of in vitro binding reactions between SRC2 bearing all three NIDs and 3-indolylmethanamines. Lane 1 shows preincubation SRC2 with **31b**. Lane 2 shows preincubation with **32a**, and lane 3 shows preincubation with vehicle only. After incubation, beads were washed and treated with VDR, and VDR–SRC2 interactions were determined by Western blot.

SRC2 interactions could be verified for all reaction conditions, although **31b**, in contrast to **32a**, was able to inhibit the interaction between VDR and SRC2 (Table 2 and Figure 8). Thus, preincubation of **31b** with SRC2 (Figure 9), in contrast to preincubation of **31b** with VDR (Figure 8), did not result in an alkylation reaction, and therefore, VDR–SRC2 binding was observed.

To examine the influence of VDR–coactivator inhibition by **31b** with respect to VDR-mediated transcription, we investigated the expression levels of the transient receptor potential vanilloid type 6 gene (*TRPV6*). The gene product of

TRPV6 (ECaC2 or CaT1) is a membrane Ca²⁺ ion channel, which is highly expressed in advanced prostate cancer²⁴ and was reported to be directly regulated by VDR in the presence of 1,25-(OH)₂D₃.²⁵ The expression levels of *TRPV6* in the prostate cancer cell line DU145 in the presence and absence of 1,25-(OH)₂D₃ and compound **31b** are depicted in Figure 10.

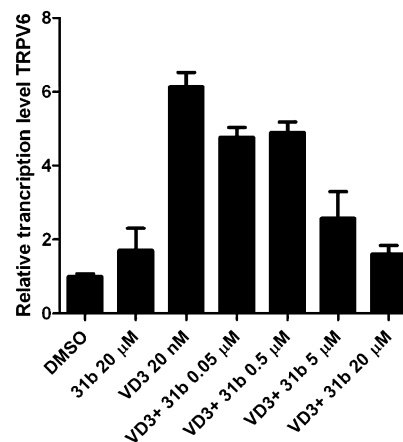


Figure 10. Modulation of expression of *TRPV6* in the presence and absence of 1,25-(OH)₂D₃ and increasing concentrations of small molecule **31b**. DU145 cells were cultured in six-well plates and treated with 1,25-(OH)₂D₃ (20 nM) and/or small molecule **31b**. *TRPV6* expression levels were determined by semiquantitative RT-PCR and normalized to GAPDH transcript level and to DMSO control condition. The $\Delta\Delta\text{Ct}$ method was used to measure the fold change in expression of genes. Standard deviations were calculated from three biological independent experiments performed in triplicate.

In the presence of 1,25-(OH)₂D₃, *TRPV6* was up-regulated in DU145 cells. The single treatment of cells with 3-indolylmethanamine **31b** at 20 μM showed no regulation of *TRPV6*. For **31b** concentrations higher than 20 μM an increased cytotoxicity was observed (see Supporting Information). In contrast, in the presence of 20 nM 1,25-(OH)₂D₃ and different concentrations of **31b**, *TRPV6* transcription was reduced in a dose dependent manner, confirming that **31b** is modulating *TRPV6* expression by interacting with VDR.

DISCUSSION

It was demonstrated that the application of HTS was successful in identifying the first irreversible inhibitors of the VDR–coactivator interactions. The screening campaign utilized a FP-based primary assay to quantify small molecule inhibition of the VDR–coactivator peptide binding. The original hit rate of 1.3% was reduced to 0.32% through the application of different scaffold filters to eliminate highly reactive molecules from the hit compound selection. These reactive molecules included enones, thiols, imines, and thioisocyanates. Rescreening of the remaining 579 compounds resulted in 140 confirmed hit compounds. Further evaluation of these molecules using secondary cell-based assays (transcription and toxicity assays) confirmed 48 compounds that exhibit biochemical and cellular activity. The purchase of these compounds as solids and screening of the freshly dissolved quality-controlled compounds using the HTS assay confirmed only 29 compounds of the initial 48 compounds. We hypothesize that the low hit reproducibility is based on at least two reasons. First is the deviation of compound activities for single point HTS assays,

and second is the limited stability of some screening compounds in DMSO.

From the selection of validated hit compounds, further characterization assays of 3-indolylmethanamines were chosen based on their promising characteristics, which included good to excellent solubility, high permeability, inhibition of VDR–SRC2-3 interaction at low micromolar concentrations, and the ability to inhibit VDR-mediated transcription in cells. In order to identify SARs for 3-indolylmethanamines, we synthesized structural analogues with diverse substituents at different positions of the scaffold. These compounds were evaluated with assays mentioned above for the initial HTS hit compounds. In general, 3-indolylmethanamines with electron donating aryl substituents inhibited the interaction between VDR and SRC2-3 coactivator peptide more quickly than 3-indolylmethanamines with electron withdrawing ones. The significance of this correlation was demonstrated with the application of a linear free energy relationship (LFER) equation, which indicated a strong and different relationship for series **30** and **31**. The negative ρ values support the hypothesized mode of binding of 3-indolylmethanamines, which includes the formation of an azafulvenium salt. This salt is then expected to react with solvent-exposed nucleophilic residue of VDR inhibiting the interaction with SRC2. The reactivity of 3-indolylmethanamines toward thiols was demonstrated by conducting FP assays in the presence of 2-mercaptoethanol, which diminished binding between VDR and compound **31b** at higher concentrations.

Many irreversible antagonists are among FDA-approved drugs, such as dibenzylamine, which is an α -adrenoceptor blocker used for hypertension. Most of these drugs are reactive toward biological nucleophilicities, but they usually exhibit high selectivities among them. An exclusive selectivity could be demonstrated for 3-indolylmethanamines in regard to their ability to disrupt the VDR–coactivator interaction in comparison with five other NR–coactivator interactions. This is remarkable because different electrophilic inhibitors (β -aminoketones and methylsulfonylnitrobenzoates) have been developed for three of these interactions (TR α –SRC2, TR β –SRC2, and PPAR γ –DRIP2).²⁶ The micromolar activity of 3-indolylmethanamine is comparable to the reported activity of direct irreversible and reversible inhibitors of other NR–coactivator interactions^{9,26} as well as to the binding affinities reported for native coactivator peptides.¹¹ Additionally, a selectivity of 3-indolylmethanamines toward the interactions between VDR–SRC2-3, VDR–SRC2-2, and VDR–DIP2 was observed among other NR–coregulator interactions tested. This is consistent with the fact that coactivator SRCs and DRIP are binding VDR at the same interaction site.²⁷

Problematic is the quantification of transcriptional inhibition for 3-indolylmethanamines because of their ability to induce cell death at a similar concentration. This resulting narrow therapeutic window is of concern for the development of nontoxic VDR–coactivator inhibitor. We hypothesize that the inhibition of transcription by itself has the potential to induce cell death including apoptosis, which has been demonstrated for TRPV6 expression by using siRNA-TRPV6.²⁸ Similar, 3-indolylmethanamine **31b** reduced the expression of TRPV6 in a dose-dependent manner as determined by rt-PCR and induced cell death at similar concentrations. Unfortunately, this antiproliferative behavior of 3-indolylmethanamines complicates the identification of transcriptional inhibition using the

described transcriptions assays because of their sensitivity toward cell toxicity.

The regulation of VDR target genes by small molecules, which includes the inhibition of VDR–coactivator interactions, represents a new strategy to develop new drug candidates for diseases related to 1,25-(OH)₂D₃ and VDR. For prostate cancer cells, for example, LNCaP cells, it was reported that 1,25-(OH)₂D₃ can induce proliferation or antiproliferation depending on the amount of supplemental serum used.²⁸ Additionally, it has been shown that the expression of TRPV6, induced by 1,25-(OH)₂D₃, is responsible for cell proliferation and apoptosis resistance.²⁹ We hypothesize that especially for prostate cancer with 1,25-(OH)₂D₃-independent proliferation (DU145), VDR antagonists such as 3-indolylmethanamines represent a new anticancer approach because of their ability to down-regulate the transcription of TRPV6 and to induce cell death.

CONCLUSION

This study reports a successful HTS strategy to identify small molecule inhibitors of VDR–coregulator interactions. To date, these are the first irreversible inhibitors of VDR–coactivator interactions that have been reported. This new class of VDR antagonists exhibits excellent selectivity among different NR–coregulator interactions and inhibits the interaction between VDR and different coactivators. This inhibition regulated the expression of VDR target genes such as TRPV6, which has been shown to be up-regulated in last stage prostate cancers. The application of 3-indolylmethanamines such as **31b** is expected to be part of new therapy to reduce prostate cancer cell growth and enables investigations toward the function of VDR–coactivator interactions during gene regulation. 3-Indolylmethanamines also have a great potential as novel drug candidates for human diseases associated with the overproduction of 1,25-(OH)₂D₃, such as sarcoidosis³⁰ or Crohn's disease.³¹ We are currently developing more selective and more potent 3-indolylmethanamines in order to study their modulation of VDR-mediated transcription and their biological activity in vivo. These future studies will include prostate cancer xenographs that enable the determination of efficacy of 3-indolylmethanamines by monitoring the expression of VDR target genes in tumors as well as the expected tumor regression. Simultaneously, any signs of acute and chronic toxicity will be determined by observation and necropsy.

EXPERIMENTAL SECTION

Chemistry. All materials were obtained from commercial suppliers and used without further purification. All solvents used were dried using an aluminum oxide column. Thin-layer chromatography was performed on precoated silica gel 60 F254 plates. Purification of compounds was carried out by normal phase column chromatography (SP1 [Biotage], silica gel 230–400 mesh) followed by evaporation. Purity determinations were performed by element analysis (EA1110, CarloErba) or using a LC–MS (Surveyor&MSQ) with a C18 column. The total flow rate was 1.0 mL/min, and the gradient program started at 90% A (0.1% formic acid in H₂O), changed to 95% B (0.1% formic acid in methanol) and then to 90% A. The mass spectrometer was operated in positive-ion mode with electrospray ionization. All compounds presented were confirmed at 95% purity or better using either method. NMR spectra are recorded on a Bruker 400 MHz and referenced internally to the residual resonance in CDCl₃ (δ 7.26 ppm for hydrogen and δ 77 ppm for carbon atoms).

General Procedure for the Aza Friedel–Crafts Reaction. In a dry flask, aniline (2 mmol) and aldehyde (2 mmol) were dissolved in

toluene (2 mL) and stirred for 1 h. Then indole (2 mmol) and decanoic acid (0.2 mmol, 10 mol %) were added slowly as a solution in toluene (2 mL). The reaction mixture was stirred at room temperature and monitored by TLC. After the reaction was completed, saturated aqueous NaHCO₃ (6 mL) was added. The mixture was extracted with dichloromethane (3 × 10 mL). The organic layer was combined, washed with brine (10 mL), and dried over anhydrous Na₂SO₄. The solvents were removed under reduced pressure, and the residue was purified by recrystallization or chromatography through Biotage SP1 flash system.

Example: N-((2-Methyl-1H-indol-3-yl)(phenyl)methyl)aniline (30a). *R_f* = 0.3 (EtOAc/hexanes = 1/4). 230 mg white solid, 37% yield. ¹H NMR (300 MHz, CDCl₃, TMS): δ 2.34 (s, 3H), 4.34 (s, 1H), 5.76 (s, 1H), 6.59 (dd, *J* = 1.8, 4.8 Hz, 2H), 6.69–6.73 (m, 1H), 6.69–7.05 (m, 1H), 7.08–7.18 (m, 4H), 7.26–7.29 (m, 3H), 7.38 (d, *J* = 7.5 Hz, 2H), 7.49 (d, *J* = 7.8 Hz, 1H), 7.82 (s, 1H). ¹³C NMR (300 MHz, CDCl₃, TMS): 12.35, 54.40, 110.8, 112.45, 113.28, 116.12, 118.76, 119.10, 120.43, 126.79, 128.58, 143.9, 144.1, 148.88, 148.96. Anal. Calcd for C₂₂H₂₀N₂: C 84.58, H 6.45, N 8.97. Found: C 84.2027, H 6.72, N 8.66.

Reagents. 1,25-(OH)₂D₃ (calcitriol) was purchased from EndoTherm, Germany. LG190178 was synthesized using a published procedure.¹²

Labeled Coregulator Peptides. Peptides, such as SRC2-3 (CLQEKHRHLKLLQNGNSPA),¹¹ were purchased and labeled with cysteine-reactive fluorophores, such as Texas-Red maleimides and Alexa Fluor 647 maleimides, in DMF/PBS, 50:50. After purification by HPLC, the corresponding labeled peptides were dissolved in DMSO and stored at –20 °C.

Protein Expression and Purification. The VDR-LBDmt DNA was kindly provided by D. Moras³³ and cloned into pMAL-c2X vector (New England Biolabs). For a detailed expression and purification protocol, see ref 11. For detailed expression and purification of protocols of PPAR γ -LBD, TR α -LBD, TR β -LBD, and AR-LBD, see ref 26b.

High Throughput FP Assay. The HTS was carried out at St. Jude Children's Research Hospital. The small molecule collection consisted of 275 000 unique compounds from commercial sources (ChemDiv, ChemBridge, and Life Chemicals). The FP assay was conducted in 384-well black polystyrene microplates (Corning, no. 3573). The assay solution contained buffer (25 mM PIPES (pH 6.75), 50 mM NaCl, 0.01% NP-40, 2% DMSO, VDR-LBD protein (1 μ M), LG190178 (5 μ M), and Alexa Fluor 647-labeled SRC2-3 (7.5 nM). Small molecule transfer into 20 μ L of assay solution was accomplished using a 50H hydrophobic coated pin tool (V&P Scientific), delivering 60 nL of a 10 mM compound solution, which resulted in a final concentration of 30 μ M. Inhibition of binding was detected using FP performed on an EnVision multilabel plate reader (GE) with a 620 nm excitation filter, a 688 nm S polarized emission filter, a 688 nm R polarized emission filter, and a Cy5 FP dichroic mirror. Automation was realized using a system developed by high resolution engineering, which uses a Stäubli T60 robot arm to transfer plates from instrument to instrument. The assay solution was dispensed in bulk into empty plates using Matrix Wellmates (Matrix Technologies), followed by compound addition, centrifugation using a Vspin plate centrifuge (Velocity 11), and incubation for 3 h at room temperature. The positive control (3-dibutylamino-1-(4-hexylphenyl)propan-1-one^{26a}) and negative control (DMSO) were measured within each plate to determine the assay plate quality and to enable data normalization.

Fluorescence Resonance Energy Transfer (FRET) Transcription Assay. A GeneBLazer (Invitrogen) assay was used to identify VDR-coactivator inhibitors that regulate VDR-mediated transcription. The provided HEK293 cells of this assay expressed a fusion protein of VDR-LBD and the GAL4-DBD, which was activated by 1,25-(OH)₂D₃, and induced transcription of a β -lactamase reporter gene. Quantification of β -lactamase was accomplished by detecting the decrease in FRET caused by the enzymatic cleavage of the β -lactam-containing substrate, which was added after an incubation time of 24 h. The cleaved substrate concentration was quantified by measuring the fluorescence emission at 447 nm. Controls for this assay were 1,25-

(OH)₂D₃ and LG190178 (positives) and DMSO (negative). Toxicity was determined by luminescence using Cell-Titer Glo (Promega), which was added to the plates after recording the FRET signal. Controls for cell viability were 3-dibutylamino-1-(4-hexylphenyl)propan-1-one (100 μ M in DMSO) (positive) and DMSO (negative). Two independent experiments were conducted in triplicate.

CYP24A1 Promoter Transcription Assay. This assay was used to determine the regulation of transcription of the VDR-target gene, CYP24A1, in the presence of small molecules. Briefly, HEK 293T cells (ATTC) were cultured in 75 cm² flasks using MEM/EBSS (Hyclone) with L-glutamine (2 mM), glucose (1 mM), nonessential amino acids, sodium pyruvate (1 mM), penicillin and streptomycin, and 10% heat inactivated FBS (Hyclone). At 50–70% confluency, cell medium was changed to phenol red free MEM/EBSS with L-glutamine (2 mM), glucose (1 mM), nonessential amino acids, sodium pyruvate (1 mM), penicillin and streptomycin, and 10% dialyzed and heat inactivated FBS (Invitrogen), followed by the addition of 2 mL of untreated MEM/EBSS containing 1.56 μ g of a VDR-pRc/CMV plasmid, 16 μ g of a luciferase reporter gene plasmid containing a rat 24-hydroxylase gene promoter (–1399 to +76), 17.4 μ g of a *Renilla* luciferase control vector (Promega), Lipofectamine LTX (75 μ L), and PLUS reagent (25 μ L). After 16 h, the cells were harvested and plated in sterile cell culture treated black 384-well plates with optical bottom (Nunc 142761) at 15 000 cells per well. After 2 h, plated cells were treated with small molecules in vehicle DMSO, followed by a 16 h incubation time. Transcription was determined using a Dual-Luciferase reporter assay (Promega). Cell viability was determined using the *Renilla* luciferase signal. IC₅₀ values and standard errors were calculated based on two independent experiments performed in quadruplicate. Controls for this assay were 1,25-(OH)₂D₃ and LG190178 (positives) and DMSO (negative). Controls for cell viability were 3-dibutylamino-1-(4-hexylphenyl)propan-1-one (100 μ M in DMSO) (positive) and DMSO (negative). Two independent experiments were conducted in quadruplicate.

VDR Ligand Competition Assay. Ligand antagonism was determined by using a FP assay (PolarScreen, Invitrogen), which employs a fluorescently labeled 1,25-(OH)₂D₃ analogue. Two independent experiments were conducted in quadruplicate, and data were analyzed using nonlinear regression with variable slope (GraphPrism).

Solubility Assay. In a 384 UV plate (Corning no. 3675), 16 compounds were serially diluted in quadruplicate starting from a 10 mM compound stock solution in DMSO. Therefore, buffer (90 mM ethanolamine, 90 mM KH₂PO₄, 90 mM potassium acetate, and 30 mM KCl (pH 7.4)) containing 20% acetonitrile was used. The plate was sealed (Corning no. 6570), sonicated for 1 min, and agitated for an additional 5 min before scanning from 230 to 800 nm at 5 min increments. A calibration plot was prepared for each compound for the maximal absorbance using background-subtracted values. A 384-well filter plate (Pall no. 5037) was prewetted with 20% acetonitrile/buffer and filled with buffer (47.5 μ L) and 10 mM compound in DMSO (2.5 μ L). The final DMSO concentration was 5%. After sonication (1 min) and agitation (12 h), the mixtures were filtered and 30 μ L of each well was transferred into a 384-well UV plate, together with the addition of 20 μ L of acetonitrile. The plate was agitated for 5 min and scanned from 230 to 800 nm at 5 min increments. The solubility was determined using background-subtracted values and the following equation: sol = (absorbance at λ_{max})/(slope)/(5/3). Each plate had the following solubility standards: 4,5-diphenylimidazole (67.3 ± 3.7 μ M), β -estradiol (43.0 ± 2.3 μ M), diethylstilbestrol (108.3 ± 5.4 μ M), ketoconazole (134.5 ± 2.4 μ M), and 3-phenylazo-2,6-diaminopyridine (357.7 ± 7.0 μ M). All experiments were conducted in quadruplicate.

Permeability Assay. This assay was carried out using Millipore's Multiscreen protocol AN172SEN00. Each plate had the following standards with the following permeability values (log *P_e*): Ranitidine (–8.02 ± 0.074 cm/s) represents low permeability. Carbamazepine (–6.81 ± 0.0011 cm/s) represents medium permeability, and verapamil (–5.93 ± 0.015 cm/s) represents high permeability. All experiments were conducted in triplet.

NR–Coactivator Binding Studies in the Presence of 3-Indolylmethamines. These assays were conducted in 384-well black polystyrene microplates (Corning) using a buffer (20 mM Tris (pH 7.50), 100 mM NaCl, 0.01% NP-40, 2% DMSO) and analyzed with a M1000 reader (Tecan) to detect FP at an excitation/emission wavelength of 595/615 nm. For the androgen receptor, AR-LBD (5 μ M), Texas Red labeled SRC2-3 (7 nM) and dihydrotestosterone (5 μ M) were incubated in buffer with small molecule for 3 h. For the thyroid receptor α , TR α -LBD (2 μ M), Texas Red labeled SRC2-2 (7 nM) and triiodothyronine (1 μ M) were incubated with small molecule for 3 h. For the thyroid receptor β , TR β -LBD (0.8 μ M), Texas Red labeled SRC2-2 (7 nM) and triiodothyronine (1 μ M) were incubated with small molecule for 3 h. For the peroxisome proliferator-activated receptor γ , PPAR γ -LBD (5 μ M), Texas Red labeled DRIP2 (7 nM) and rosiglitazone (5 μ M) were incubated with small molecule for 3 h. For the VDR, VDR-LBD (1 μ M), Texas Red labeled SRC2-3 (7 nM) and LG190178 (5 μ M) were incubated with small molecule for 3 h. Two independent experiments were carried out in quadruplicate, and data were analyzed using nonlinear regression with variable slope (GraphPrism).

VDR–Coactivator Binding Studies in the Presence of 3-Indolylmethamine 31b. These assays were conducted in 384-well black polystyrene microplates (Corning) using a buffer (25 mM PIPES (pH 6.75), 50 mM NaCl, 0.01% NP-40, 2% DMSO) and analyzed with a M1000 reader (Tecan) to detect FP at an excitation/emission wavelength of 595/615 nm. VDR-LBD protein (1 μ M), LG190178 (5 μ M), and 7.5 nM Texas Red labeled SRC1-3 [CESKDHQLLRYLLDKDEKDL], Texas Red labeled SRC2-3 [CLQEKH-RILHKLLQNGNSPA], Texas Red labeled SRC3-3 [CKKENNALLRYLLDRDDPSD], or Texas Red labeled DRIP2 [CNTKNHPMLMNLKDNPAQD] were incubated with different concentration of 31b. Two independent experiments were carried out in quadruplicate, and data were analyzed using nonlinear regression with variable slope (GraphPrism).

Western Blot of in Vitro Binding Reactions between SRC2 Bearing All Three NIDs and VDR-LBD in the Presence of 31b. GST fusion to the SRC2 bearing all three NIDs was expressed in *Escherichia coli* BL21. Cultures were grown to OD₆₀₀ = 0.5–0.6 at 22 °C and induced with 0.5 mM isopropyl-D-thiogalactoside for 12 h. The cultures were centrifuged (1000g), and bacterial pellets were resuspended in 20 mM Tris, pH 7.4, 200 mM NaCl, 1 mM Na₃N, 0.5 M EDTA, 1 mM DTT, protein inhibitors cocktail (Roche) and sonicated. Debris was pelleted by centrifugation (100000g). The supernatant was incubated with glutathione-Sepharose 4B beads (Amersham Biosciences) and washed. Protein on bead was stored with 10% glycerol at –20 °C. Each pull-down reaction was carried out in 100 μ L of buffer (25 mM PIPES (pH 6.75), 50 mM NaCl, 0.01% NP-40, 2% DMSO) using 100 nM calcitriol, 10 μ M VDR-LBD-MPB, and 31b. After 2 h at rt, 15 μ L of SRC2-beads was added to each reaction followed by 30 min of incubation. The mixture was filtered, washed with buffer (100 μ L), and eluted from the bead using a buffer and 10 mM reduced glutathione. Separation was carried out using SDS–PAGE followed by Western blotting using standard procedures with anti-MBP (E8032S, New England BioLabs) and anti-mouse IgG-Tr (sc-2781, Santa Cruz, CA).

Semiquantitative Real Time PCR. DU145 cells were incubated at 37 °C with 31b (20 μ M) in the presence or absence of 20 nM calcitriol for 18 h. Total RNA was isolated from cells using an RNAeasy kit (Qiagen). Genomic DNA was removed, and cDNA was generated using equal amounts of RNA (QuantiTect reverse transcription kit, Qiagen). The cDNA mixture was then diluted 5-fold, and the QuantiFast SYBR Green PCR kit (Qiagen) was used for the real time PCR following manufacturer's recommendations. Primers used in these studies are as follows: GAPDH forward primer 5-accacagtcctccatcac-3, reverse primer 5-tccaccacctgtgctgta-3; TRPV6 FP 5-ACTGTCATTGGGGCTATCATC-3, RP 5-CAGCA-GAATCGCATCAGGTC-3. rReal-time rt-PCR was carried out on a Mastercycler (Eppendorf). We used the $\Delta\Delta$ Ct method to measure the fold change in gene expression of target genes. Standard deviations

were calculated from three biological independent experiments performed in triplicate.

■ ASSOCIATED CONTENT

§ Supporting Information

Inhibition of VDR–SRC2-3 binding in the presence of 3-dibutylamino-1-(4-hexylphenyl)propan-1-one, synthesis and characterization of molecules, graphical representation of rate constants, nuclear receptor–coactivator binding isotherms, and VDR–ligand competition isotherms. This material is available free of charge via the Internet at <http://pubs.acs.org>.

■ AUTHOR INFORMATION

Corresponding Author

*Phone: (414) 229 2612. Fax: (414) 229 5530. E-mail: arnold2@uwm.edu.

Author Contributions

^{||}Both authors contributed equally to this work.

Notes

The authors declare no competing financial interest.

■ ACKNOWLEDGMENTS

We thank Taosheng Chen, Fu-Yue Zeng, Wenwei Lin, and Jimmy Cui for their assistance with the HTS at the St. Jude High Throughput Screening Center, as well as Aaron Kosinski for his assistance with protein preparation. We also thank Paul Webb and Phuong Nguyen for providing us with the SRC2 plasmid. This work was supported by the University of Wisconsin-Milwaukee (L.A.A.), NIH Grants DA031090 (L.A.A.) and DK58080 (R.K.G.), the American Lebanese Syrian Associated Charities (ALSAC) (R.K.G.), and St. Jude Children's Research Hospital (R.K.G.).

■ ABBREVIATIONS USED

VDR, vitamin D receptor; NR, nuclear hormone receptor; FP, fluorescence polarization; SRC2, steroid receptor coactivator 2; SRC2-3, labeled steroid receptor coactivator 2 peptide; SAR, structure–activity relationship; TRPV6, transient receptor potential vanilloid type 6 gene; 1,25-(OH)₂D₃, 1,25-dihydroxyvitamin D₃; DBD, DNA binding domain; LBD, ligand-binding domain; RXR, retinoid X receptor; HTS, high throughput screening; DMSO, dimethyl sulfoxide; HEK293, human embryonic kidney cell; FRET, fluorescence resonance energy transfer; LC–MS, liquid chromatography–mass spectrometry; PAMPA, parallel artificial membrane permeability; AR, androgen receptor; ER β , estrogen receptor β ; TR α , thyroid receptor α ; TR β , thyroid receptor β ; PPAR γ , peroxisome proliferator-activated receptor γ ; DRIP205, vitamin D receptor interacting protein 205; GST, glutathione S-transferase; DU145, human prostate cancer cell; GAPDH, glyceraldehyde 3-phosphate dehydrogenase; LFER, linear free energy relationship

■ REFERENCES

- Brumbaugh, P. F.; Haussler, M. R. 1 Alpha,25-dihydroxycholecalciferol receptors in intestine. I. Association of 1 alpha,25-dihydroxycholecalciferol with intestinal mucosa chromatin. *J. Biol. Chem.* **1974**, *249*, 1251–1257.
- Jurutka, P. W.; Whitfield, G. K.; Hsieh, J. C.; Thompson, P. D.; Haussler, C. A.; Haussler, M. R. Molecular nature of the vitamin D receptor and its role in regulation of gene expression. *Rev. Endocr. Metab. Disord.* **2001**, *2*, 203–216.

- (3) Feldman, D.; Pike, J. W.; Glorieux, F. H. *Vitamin D*, 2nd ed.; Elsevier: Burlington, VT, 2005; Vol. 1–2.
- (4) Yamada, S.; Shimizu, M.; Yamamoto, K. Vitamin D receptor. *Endocr. Dev.* **2003**, *6*, 50–63.
- (5) Toell, A.; Polly, P.; Carlberg, C. All natural DR3-type vitamin D response elements show a similar functionality in vitro. *Biochem. J.* **2000**, *352* (Part2), 301–309.
- (6) Kim, J. Y.; Son, Y. L.; Lee, Y. C. Involvement of SMRT corepressor in transcriptional repression by the vitamin D receptor. *Mol. Endocrinol.* **2009**, *23*, 251–264.
- (7) Rachez, C.; Freedman, L. P. Mechanisms of gene regulation by vitamin D(3) receptor: a network of coactivator interactions. *Gene* **2000**, *246*, 9–21.
- (8) (a) Lamblin, M.; Spingarn, R.; Wang, T. T.; Burger, M. C.; Dabbas, B.; Moitessier, N.; White, J. H.; Gleason, J. L. An *o*-aminoanilide analogue of 1 α ,25-dihydroxyvitamin D(3) functions as a strong vitamin D receptor antagonist. *J. Med. Chem.* **2010**, *53*, 7461–7465. (b) Kato, Y.; Nakano, Y.; Sano, H.; Tanatani, A.; Kobayashi, H.; Shimazawa, R.; Koshino, H.; Hashimoto, Y.; Nagasawa, K. Synthesis of 1 α ,25-dihydroxyvitamin D₃-26,23-lactams (DLAMs), a novel series of 1 α ,25-dihydroxyvitamin D₃ antagonist. *Bioorg. Med. Chem. Lett.* **2004**, *14*, 2579–2583. (c) Inaba, Y.; Yoshimoto, N.; Sakamaki, Y.; Nakabayashi, M.; Ikura, T.; Tamamura, H.; Ito, N.; Shimizu, M.; Yamamoto, K. A new class of vitamin D analogues that induce structural rearrangement of the ligand-binding pocket of the receptor. *J. Med. Chem.* **2009**, *52*, 1438–1449. (d) Nakabayashi, M.; Yamada, S.; Yoshimoto, N.; Tanaka, T.; Igarashi, M.; Ikura, T.; Ito, N.; Makishima, M.; Tokiwa, H.; DeLuca, H. F.; Shimizu, M. Crystal structures of rat vitamin D receptor bound to adamantyl vitamin D analogs: structural basis for vitamin D receptor antagonism and partial agonism. *J. Med. Chem.* **2008**, *51*, 5320–5329. (e) Saito, N.; Kittaka, A. Highly potent vitamin D receptor antagonists: design, synthesis, and biological evaluation. *ChemBioChem* **2006**, *7*, 1479–1490. (f) Cho, K.; Uneuchi, F.; Kato-Nakamura, Y.; Namekawa, J.; Ishizuka, S.; Takenouchi, K.; Nagasawa, K. Structure–activity relationship studies on vitamin D lactam derivatives as vitamin D receptor antagonist. *Bioorg. Med. Chem. Lett.* **2008**, *18*, 4287–4290. (g) Herdick, M.; Steinmeyer, A.; Carlberg, C. Antagonistic action of a 25-carboxylic ester analogue of 1 α , 25-dihydroxyvitamin D₃ is mediated by a lack of ligand-induced vitamin D receptor interaction with coactivators. *J. Biol. Chem.* **2000**, *275*, 16506–16512. (h) Ishizuka, S.; Kurihara, N.; Miura, D.; Takenouchi, K.; Cornish, J.; Cundy, T.; Reddy, S. V.; Roodman, G. D. Vitamin D antagonist, TEI-9647, inhibits osteoclast formation induced by 1 α ,25-dihydroxyvitamin D₃ from pagetic bone marrow cells. *J. Steroid Biochem. Mol. Biol.* **2004**, *89*–90, 331–334.
- (9) Moore, T. W.; Katzenellenbogen, J. A. Inhibitors of nuclear hormone receptor/coactivator interactions. *Annu. Rep. Med. Chem.* **2009**, *44*, 443–457.
- (10) Mita, Y.; Dodo, K.; Noguchi-Yachide, T.; Miyachi, H.; Makishima, M.; Hashimoto, Y.; Ishikawa, M. LXXLL peptide mimetics as inhibitors of the interaction of vitamin D receptor with coactivators. *Bioorg. Med. Chem. Lett.* **2010**, *20*, 1712–1717.
- (11) Teichert, A.; Arnold, L. A.; Otieno, S.; Oda, Y.; Augustinaite, I.; Geistlinger, T. R.; Kriwacki, R. W.; Guy, R. K.; Bikle, D. D. Quantification of the vitamin D receptor–coregulator interaction. *Biochemistry* **2009**, *48*, 1454–1461.
- (12) Boehm, M. F.; Fitzgerald, P.; Zou, A.; Elgort, M. G.; Bischoff, E. D.; Mere, L.; Mais, D. E.; Bissonnette, R. P.; Heyman, R. A.; Nadzan, A. M.; Reichman, M.; Allegretto, E. A. Novel nonsteroidal vitamin D mimics exert VDR-modulating activities with less calcium mobilization than 1,25-dihydroxyvitamin D₃. *Chem. Biol.* **1999**, *6*, 265–275.
- (13) Arnold, L. A.; Kosinski, A.; Estebanez-Perpina, E.; Fletterick, R. J.; Guy, R. K. Inhibitors of the interaction of a thyroid hormone receptor and coactivators: preliminary structure–activity relationships. *J. Med. Chem.* **2007**, *50*, 5269–5280.
- (14) McGovern, S. L.; Caselli, E.; Grigorieff, N.; Shoichet, B. K. A common mechanism underlying promiscuous inhibitors from virtual and high-throughput screening. *J. Med. Chem.* **2002**, *45*, 1712–1722.
- (15) Huth, J. R.; Song, D.; Mendoza, R. R.; Black-Schaefer, C. L.; Mack, J. C.; Dorwin, S. A.; Lador, U. S.; Severin, J. M.; Walter, K. A.; Bartley, D. M.; Hajduk, P. J. Toxicological evaluation of thiol-reactive compounds identified using a la assay to detect reactive molecules by nuclear magnetic resonance. *Chem. Res. Toxicol.* **2007**, *20*, 1752–1759.
- (16) Chen, K. S.; DeLuca, H. F. Cloning of the human 1 α ,25-dihydroxyvitamin D₃ 24-hydroxylase gene promoter and identification of two vitamin D-responsive elements. *Biochim. Biophys. Acta* **1995**, *1263*, 1–9.
- (17) Holick, M. F.; Kleiner-Bossaller, A.; Schnoes, H. K.; Kasten, P. M.; Boyle, I. T.; DeLuca, H. F. 1,24,25-Trihydroxyvitamin D₃. A metabolite of vitamin D₃ effective on intestine. *J. Biol. Chem.* **1973**, *248*, 6691–6696.
- (18) Xie, W. H.; Bloomfield, K. M.; Jin, Y. F.; Dolney, N. Y.; Wang, P. G. Lanthanide triflates catalyzed reactions of imines with indole in protic media. *Synlett* **1999**, 498–500.
- (19) Ritchie, C. D.; Sager, W. F. An examination of structure–activity relationships. *Prog. Phys. Org. Chem.* **1964**, *2*, 323–400.
- (20) (a) Estebanez-Perpina, E.; Moore, J. M.; Mar, E.; Delgado-Rodriguez, E.; Nguyen, P.; Baxter, J. D.; Buehrer, B. M.; Webb, P.; Fletterick, R. J.; Guy, R. K. The molecular mechanisms of coactivator utilization in ligand-dependent transactivation by the androgen receptor. *J. Biol. Chem.* **2005**, *280*, 8060–8068. (b) Moore, J. M.; Galicia, S. J.; McReynolds, A. C.; Nguyen, N. H.; Scanlan, T. S.; Guy, R. K. Quantitative proteomics of the thyroid hormone receptor–coregulator interactions. *J. Biol. Chem.* **2004**, *279*, 27584–27590.
- (21) (a) Masuyama, H.; Brownfield, C. M.; St-Arnaud, R.; MacDonald, P. N. Evidence for ligand-dependent intramolecular folding of the AF-2 domain in vitamin D receptor-activated transcription and coactivator interaction. *Mol. Endocrinol.* **1997**, *11*, 1507–1517. (b) Hong, H.; Kohli, K.; Garabedian, M. J.; Stallcup, M. R. GRIP1, a transcriptional coactivator for the AF-2 transactivation domain of steroid, thyroid, retinoid, and vitamin D receptors. *Mol. Cell. Biol.* **1997**, *17*, 2735–2744. (c) Li, H.; Gomes, P. J.; Chen, J. D. RAC3, a steroid/nuclear receptor-associated coactivator that is related to SRC-1 and TIF2. *Proc. Natl. Acad. Sci. U.S.A.* **1997**, *94*, 8479–8484.
- (22) Rachez, C.; Suldan, Z.; Ward, J.; Chang, C. P.; Burakov, D.; Erdjument-Bromage, H.; Tempst, P.; Freedman, L. P. A novel protein complex that interacts with the vitamin D₃ receptor in a ligand-dependent manner and enhances VDR transactivation in a cell-free system. *Genes Dev.* **1998**, *12*, 1787–1800.
- (23) Hsieh, J. C.; Sisk, J. M.; Jurutka, P. W.; Haussler, C. A.; Slater, S. A.; Haussler, M. R.; Thompson, C. C. Physical and functional interaction between the vitamin D receptor and hairless corepressor, two proteins required for hair cycling. *J. Biol. Chem.* **2003**, *278*, 38665–38674.
- (24) (a) Wissenbach, U.; Niemeyer, B.; Himmerkus, N.; Fixemer, T.; Bonkhoff, H.; Flockerzi, V. TRPV6 and prostate cancer: cancer growth beyond the prostate correlates with increased TRPV6 Ca²⁺ channel expression. *Biochem. Biophys. Res. Commun.* **2004**, *322*, 1359–1363. (b) Nijenhuis, T.; Hoenderop, J. G.; van der Kemp, A. W.; Bindels, R. J. Localization and regulation of the epithelial Ca²⁺ channel TRPV6 in the kidney. *J. Am. Soc. Nephrol.* **2003**, *14*, 2731–2740.
- (25) Meyer, M. B.; Watanuki, M.; Kim, S.; Shevde, N. K.; Pike, J. W. The human transient receptor potential vanilloid type 6 distal promoter contains multiple vitamin D receptor binding sites that mediate activation by 1,25-dihydroxyvitamin D₃ in intestinal cells. *Mol. Endocrinol.* **2006**, *20*, 1447–1461.
- (26) (a) Arnold, L. A.; Estebanez-Perpina, E.; Togashi, M.; Jouravel, N.; Shelat, A.; McReynolds, A. C.; Mar, E.; Nguyen, P.; Baxter, J. D.; Fletterick, R. J.; Webb, P.; Guy, R. K. Discovery of small molecule inhibitors of the interaction of the thyroid hormone receptor with transcriptional coregulators. *J. Biol. Chem.* **2005**, *280*, 43048–43055. (b) Hwang, J. Y.; Huang, W.; Arnold, L. A.; Huang, R.; Attia, R. R.; Connelly, M.; Wichterman, J.; Zhu, F.; Augustinaite, I.; Austin, C. P.; Ingles, J.; Johnson, R. L.; Guy, R. K. Methylsulfonylnitrobenzoates, a

new class of irreversible inhibitors of the interaction of the thyroid hormone receptor and its obligate coactivators that functionally antagonizes thyroid hormone. *J. Biol. Chem.* **2011**, *286*, 11895–11908.

(27) (a) Ciesielski, F.; Rochel, N.; Moras, D. Adaptability of the Vitamin D nuclear receptor to the synthetic ligand Gemini: remodelling the LBP with one side chain rotation. *J. Steroid Biochem. Mol. Biol.* **2007**, *103*, 235–242. (b) Vanhooke, J. L.; Benning, M. M.; Bauer, C. B.; Pike, J. W.; DeLuca, H. F. Molecular structure of the rat vitamin D receptor ligand binding domain complexed with 2-carbon-substituted vitamin D₃ hormone analogues and a LXXLL-containing coactivator peptide. *Biochemistry* **2004**, *43*, 4101–4110.

(28) Lehen'kyi, V.; Raphael, M.; Oulidi, A.; Flourakis, M.; Khalimonchik, S.; Kondratskiy, A.; Gordienko, D. V.; Mauroy, B.; Bonnal, J. L.; Skryma, R.; Prevarskaya, N. TRPV6 determines the effect of vitamin D₃ on prostate cancer cell growth. *PLoS One* **2011**, *6*, e16856.

(29) Lehen'kyi, V.; Flourakis, M.; Skryma, R.; Prevarskaya, N. TRPV6 channel controls prostate cancer cell proliferation via Ca²⁺/NFAT-dependent pathways. *Oncogene* **2007**, *26*, 7380–7385.

(30) Stern, P. H.; De Olazabal, J.; Bell, N. H. Evidence for abnormal regulation of circulating 1 alpha,25-dihydroxyvitamin D in patients with sarcoidosis and normal calcium metabolism. *J. Clin. Invest.* **1980**, *66*, 852–855.

(31) Bosch, X. Hypercalcemia due to endogenous overproduction of 1,25-dihydroxyvitamin D in Crohn's disease. *Gastroenterology* **1998**, *114*, 1061–1065.

(32) Shirakawa, S.; Kobayashi, S. Carboxylic acid catalyzed three-component aza-Friedel–Crafts reactions in water for the synthesis of 3-substituted indoles. *Org. Lett.* **2006**, *8*, 4939–4942.

(33) Rochel, N.; Wurtz, J. M.; Mitschler, A.; Klaholz, B.; Moras, D. The crystal structure of the nuclear receptor for vitamin D bound to its natural ligand. *Mol. Cell* **2000**, *5*, 173–179.